Biomaterials 32 (2011) 8218–8225

Contents lists available at ScienceDirect

Biomaterials

journal homepage: www.elsevier.com/locate/biomaterials

The role of the tumor suppressor p53 pathway in the cellular DNA damage response to zinc oxide nanoparticles

Kee Woei Ng [a], Stella P.K. Khoo [b], Boon Chin Heng [a], Magdiel I. Setyawati [c], Eng Chok Tan [b], Xinxin Zhao [a], Sijing Xiong [a], Wanru Fang [d], David T. Leong [c,d,*], Joachim S.C. Loo [a,**]

[a] School of Materials Science and Engineering, Nanyang Technological University, 50 Nanyang Avenue, Singapore 639798, Singapore
[b] School of Biological Sciences, Nanyang Technological University, 60 Nanyang Drive, Singapore 637551, Singapore
[c] Department of Chemical & Biomolecular Engineering, National University of Singapore, 4 Engineering Drive 4, Singapore 117576, Singapore
[d] Cancer Science Institute of Singapore, National University of Singapore, 28 Medical Drive, Singapore 117456, Singapore

ARTICLE INFO

Article history:
Received 2 June 2011
Accepted 11 July 2011
Available online 31 July 2011

Keywords:
Nanotoxicology
Genotoxicology
Zinc oxide
Nanoparticles
DNA damage
p53

ABSTRACT

In this paper, we explored how ZnO nanoparticles cross-interact with a critical tumor suppressive pathway centered around p53, which is one of the most important known tumor suppressors that protects cells from developing cancer phenotypes through its control over major pathways like apoptosis, senescence and cell cycle progression. We showed that the p53 pathway was activated in BJ cells (skin fibroblasts) upon ZnO nanoparticles treatment with a concomitant decrease in cell numbers. This suggests that cellular responses like apoptosis in the presence of ZnO nanoparticles require p53 as the molecular master switch towards programmed cell death. This also suggests that in cells without robust p53, protective response can be tipped towards carcinogenesis when stimulated by DNA damage inducing agents like ZnO nanoparticles. We observed this precarious tendency in the same BJ cells with p53 knocked down using endogeneous expressing shRNA. These p53 knocked down BJ cells became more resistant to ZnO nanoparticles induced cell death and increased cell progression. Collectively, our results suggest that cellular response towards specific nanoparticle induced cell toxicity and carcinogenesis is not only dependent on specific nanoparticle properties but also (perhaps more importantly) the endogenous genetic, transcriptomic and proteomic landscape of the target cells.

1. Introduction

Nanotoxicology, or the study of potential ill-effects of nanomaterials on the human body, has grown in significance over recent years [1–3] fueled by the surge in the number of nanomaterial-based consumer products in the market. The nanotechnology consumer products inventory maintained by the Project on Emerging Nanotechnologies (PEN) contained 1015 nanomaterial-based consumer products as of August 2009, representing a massive increase of 379% since March 2006 [4]. Although it is important to understand and highlight the potential ill-effects of nanomaterials, it is equally important that nanotoxicology does not become a stumbling block in the development of nanotechnologies that can benefit mankind in areas such as healthcare. The key is therefore to accelerate our scientific understanding of nanomaterial interactions with biological systems in order for regulatory bodies to map out the guidelines governing the use of nanomaterials in consumer products – a point that has been repeatedly highlighted by professional groups such as the Scientific Committee on Emerging and Newly Identified Health Risks (SCENIHR, European Commission) [5]. Zinc oxide (ZnO) nanoparticles are amongst the most commonly utilized nanomaterials in consumer products, most notably in sunscreens because of their superior efficiency in absorbing UV [6,7]. It has also been suggested that ZnO nanoparticles can be developed as an alternative anticancer therapeutic agent because of their cancer cell targeting potential [8], and potential for multimodal cancer treatment [9]. More recently, ZnO nanoparticles are also being developed as bioimaging probes [10–12] and drug delivery vehicles [10,13]. However, there are ample reports in the literature documenting the cytotoxic effects of ZnO nanoparticles *in vitro* [14–17]. Concerns are also rising with respect to the possible genotoxic effects of these particles [18,19], due to their potential devastating long term

* Corresponding author. Department of Chemical & Biomolecular Engineering, National University of Singapore, 4 Engineering Drive 4, Singapore 117576, Singapore. Tel.: +65 6516 7262; fax: +65 6779 1936.
** Corresponding author. Tel.: +65 6790 4603; fax: +65 6790 9081.
E-mail addresses: csiltwd@nus.edu.sg, cheltwd@nus.edu.sg (D.T. Leong), joachimloo@ntu.edu.sg, joachimloo@hotmail.com (J.S.C. Loo).

0142-9612/$ – see front matter © 2011 Elsevier Ltd. All rights reserved.
doi:10.1016/j.biomaterials.2011.07.036

damage caused to humans. To this end, we examined the genotoxic influence exerted by ZnO nanoparticles on mammalian cells.

A typical cell is constantly bombarded by many possible events that damage its DNA. Events include ionizing radiation, ultraviolet light, chemical agents like methyl methanesulfonate, cisplatin and mitomycin C. Cigarette smoking derived adducts and oxidizing agents [20] account for the astonishing level of 10^5 DNA lesions experienced in a cell per day [21]. The cell responds to DNA damage by first attempting to repair the damage. If the DNA damage is irreparable, it either undergoes apoptosis (programmed cell death) or senescence (aging). This is to prevent any damaged DNA progressing to deleterious mutations that would be passed down to its progeny. Any dysfunction in all these defensive mechanisms can lead to uncontrollable proliferation which ultimately presents itself as cancer. Tumor suppressors are key sentinel genes that ensure correct functioning of the defensive mechanisms. p53 is one such tumor suppressor that has been extensively studied in cancer biology due to its importance in regulating cellular responses to genotoxic and cytotoxic effects. It is considered to be the central sentinel transcription factor that controls the apoptotic and senescence pathways arising from cells experiencing irreparable DNA damage and has been found to be non-functional in almost all cancer types [22,23]. p53 is endogenously expressed but is quickly degraded upon MDM2 binding [23]. However, when activated, p53 gets phosphorylated and that prevents its degradation. Phosphorylated p53 then transcribes a long list of important apoptotic and senescence genes. Another key tumor suppressor, retinoblastoma protein (Rb) exerts its role in inhibiting G1-S cell cycle progression. Rb binds and inhibits E2F, a class of transcription factors whose targets are largely involved in promoting cell cycle progression. Phosphorylated Rb decouples from E2F, resulting essentially in removing its inhibitory effects on E2F. The net outcome is cell cycle progression.

To deeper understand the toxicity effects exerted by ZnO nanoparticles, we therefore asked a fundamental and biologically significant question of whether the cellular DNA damage pathway, through tumor suppressor p53, is activated by ZnO nanoparticles. Ahamed et al. [24] demonstrated recently that there was upregulation of p53 when A549 cells were treated with ZnO nanorods. However, upregulation of p53 could be a side effect of ZnO nanorods treatment that may not be linked to cell death. To prove that cell death caused by ZnO treatment does go through p53, one needs to remove p53 function and show that the effect caused by ZnO nanoparticles is curtailed. Nonetheless, it is difficult to do this in leukemia cancer derived or SV-40 large T-antigen transformed cells like RAW264.7 [25] and BEAS-2B [26] respectively due to their dysfunctional p53 pathway [27]. In order to study the role of p53 with more certainty, we therefore turned to a human skin fibroblast cell line (BJ) that has more defined genotypes versus the typical use of cancer cell lines [28]. The BJ cell line is also amenable to introduction of specific genetic changes for more controlled experimental setup [29]. Wild type BJ cells (WT p53) retain a functional p53 pathway and is responsive to DNA damage response through p53 [30]. In this study, we knocked down p53 in BJ cells (shp53) in order to evaluate the role that p53 plays in ZnO nanoparticles induced DNA damage.

2. Materials and methods

2.1. Characterization of ZnO nanoparticles

ZnO nanoparticles were purchased from Meliorium Technologies Inc. (Rochester, NY, USA). To evaluate particle size and morphology, ZnO nanoparticles were observed under transmission electron microscopy (TEM; Jeol 2010) at an accelerating voltage of 200 kV with a LaB6 cathode. Samples were prepared by mixing a small quantity of nanoparticles in methanol followed by 30 min of ultrasonic treatment, and then dropped on carbon coated copper grids. Nanoparticle samples were measured for size from their TEM micrographs using the ImageJ software. Dynamic light scattering (DLS) (Malvern Co., UK) was utilized to test the hydrodynamic size, polydispersity index (PDI) and zeta potential of the particles. Prior to test, the nanoparticle samples were dispersed and ultrasonicated in Milli-Q water (pH = 6) for 5 min to form colloidal suspensions. Each sample was tested in triplicates and the mean values were reported.

2.2. Cell culture

Human bronchial epithelial cells (BEAS-2B), human neonatal foreskin fibroblasts (BJ) and murine macrophages (RAW264.7) were purchased from the American Type Culture Collection (ATCC, Manassas, VA, USA). All 3 cell types were cultured in complete DMEM (high glucose Dulbecco's Modified Eagle's Media; PAA Laboratories Inc., MA, USA) supplemented with 10% FBS, 1% L-glutamine and 1% Antibiotics/Antimycotics (PAA Laboratories Inc.) at standard culture conditions (37 °C, 5% CO_2) and sub-cultured in the ratio of 1:2 to 1:4 at 90% confluency.

2.3. Packaging shp53 retrovirus and transduction of BJ cells

EcoPack^{Tm} 2-293 (Clontech, CA, USA) cells at 70% confluency were transfected by calcium phosphate method with retroviral plasmids encoding either shp53 [31] or empty vector control. Cells were washed with sterile PBS after 12 h of transfection. Virus containing media was collected and clarified 48 h after transfection and stored at −80 °C. BJ cells expressing the ecotropic receptor were plated at 70% confluence the evening before transduction. Equal volumes of viral media were mixed with growth media containing polybrene (8 μg/ml final concentration) and added directly to cells. Cells were selected with 2 μg/ml blasticidine for positively transduced cells for one week.

2.4. Exposure of cells to nanoparticles

Stock solutions of ZnO nanoparticles were prepared in sterile PBS (PAA Laboratories Inc.), sterilized by UV exposure for 15 min and bath sonicated for 10 min. These were added to complete DMEM (10% nanoparticles in PBS in 90% complete DMEM) and further bath sonicated for 10 min to make up the final concentrations of nanoparticles required: 5, 10, 15, 20, 25 μg/ml. For cytotoxic analysis, BEAS-2B and RAW264.7 cells were cultured at 50,000 cells/cm^2 in 24-well plate format (Corning Inc., NY, USA) for 24 h prior to nanoparticle exposure. For studying genotoxic effects of nanoparticles, BJ cells were first cultured at 13,000 cells/cm^2 in 6-well plate format (Corning Inc.) overnight and then serum-starved for 24 h before exposure to the nanoparticles. The media were then replaced with freshly prepared nanoparticle suspensions at the appropriate concentrations in standard culture conditions. The suspensions were replaced every two days. Untreated cells cultured in complete DMEM containing 10% PBS as vehicle control served as the negative controls.

2.5. Cell proliferation and metabolic profile

To measure cell proliferation by quantifying DNA amounts, nanoparticle-treated cells were washed thrice in PBS at the appropriate time points and lysed with 0.5 ml per well of 0.1% (v/v) Triton X-100 in deionized water for 30 min with agitation at 80 rpm. The PicoGreen® working solution (Invitrogen, CA, USA) was prepared according to the manufacturer's instructions and mixed with the cell lysates in 1:1 ratio in 96-well plate formats. Samples were incubated for 5 min at room temperature in the dark before fluorescence was recorded using a microplate reader (Infinite 200, Tecan Inc., Maennedorf, Switzerland) at an excitation wavelength of 480 nm and emission wavelength of 520 nm. The relative percentage of viable cells was obtained by normalizing the fluorescence values of the nanoparticles-treated cells to the negative controls (untreated cells). For the analysis of cell metabolic profiles, nanoparticles-treated cells were washed thrice in PBS and administered 0.5 ml per well of serum-free DMEM without phenol red, containing 10% WST-8 reagent (Dojindo Molecular Laboratories Inc., Japan). Cells were incubated at standard culture conditions for 2 h and 100 μl of the reaction mixture from each well was then transferred onto fresh 96-well plates (Corning Inc.). Absorbance readings were recorded at 450 nm using a Tecan Infinite 200 microplate reader (Tecan Inc., Maennedorf, Switzerland). The relative metabolic profiles of cultures were obtained by normalizing the WST-8 absorbance values to DNA amount quantified with the PicoGreen® assay.

2.6. Comet assay

Comet assay was carried out as described previously [32], with slight modifications. BEAS-2B cells were seeded at 5000 cells/cm^2 and incubated for 16 h. Nanoparticles were then added as described earlier and incubated for 4 h. Subsequently, cells were rinsed with PBS, trypsinized and mixed with 1% low gelling temperature agarose (Bio-rad, CA, USA) at a ratio of 1:3. The cell-agarose suspension was spread evenly across an agarose pre-coated glass slide and allowed to gel for 5 min at 4 °C. This was then placed in a lysis solution (1.2 M NaCl, 100 mM EDTA, 1% Triton X, 0.26 M NaOH) for 16 h in the dark at 4 °C before carrying out the

electrophoresis at 10V, 18 mA for 25 min in the dark. The slides were then washed with distilled water, stained with 1:2500 dilution from stock SYBR Green (Sigma–Aldrich, MO, USA) for 20 min in the dark at 4 °C and viewed under a fluorescence microscope (Nikon Eclipse 80i, Japan). For each slide, 50 cells were scored using TriTek CometScore™ (www.autocomet.com).

2.7. Western blotting

Cells were washed thrice with PBS and lysed with 50 μl of sample buffer (31.25 mM Tris–HCl, pH 6.8, 12.5% glycerol, 0.05% β-mercaptoethanol, 1% SDS, 0.005% bromophenol blue) supplemented with protease inhibitors and phosphatase inhibitor cocktail (Sigma–Aldrich). Cell lysates were harvested on ice, sonicated briefly and centrifuged at 10,000 g for 10 min at 4 °C to remove cell debris. Protein concentrations of the collected supernatants were measured using the 660 nm protein assay kit with the proprietary Ionic Detergent Compatibility Reagent (IDCR) (Thermo Scientific, IL, USA). Samples of 7 μg total protein were boiled for 10 min prior to SDS- polyacrylamide gel electrophoresis (PAGE) using 4–12% gradient gels (NuPAGE®, Invitrogen) at 120 V for 90 min. Thereafter, gels were electrotransferred using the iBlot® dry blotting system onto nitrocellulose membranes (Invitrogen). Immunoblotting of the membranes was done by first blocking unspecific sites with 5% (w/v) filtered non-fat dry milk in TBS-T (50 mM Tris–HCl pH 7.2, 150 mM NaCl, 0.03% (v/v) Tween-20), for 30 min at room temperature. Membranes were probed with primary antibodies diluted in wash buffer containing 3% (w/v) BSA or 3% (w/v) milk and incubated overnight at 4 °C with gentle agitation. After washing thrice with wash buffer, blots were incubated with HRP-conjugated secondary antibodies diluted 1:4000 in the respective blocking solutions, for 30 min at room temperature. Protein bands were visualized with SuperSignal West Pico Chemiluminescent substrate (Thermo Scientific) using gel documentation system (LAS-4000, GE Healthcare, UK). The primary antibodies used were rabbit anti-phosphorylated Rb (Ser 807/811 - #9301; Cell Signalling Technology, USA), mouse anti-phosphorylated p53 (Ser15 - #9286; Cell Signalling Technology), mouse anti-Rb (sc-74562; Santa Cruz, USA), rabbit anti-p53 (sc-6243; Santa Cruz, USA) and mouse anti-β-actin (sc-47778; Santa Cruz, USA). The secondary antibodies used were HRP-conjugated goat anti-mouse IgG antibody (P0447, Dako, Denmark) and HRP-conjugated goat anti-rabbit IgG antibody (P0448, Dako, Denmark).

2.8. Statistical analysis

All quantitative data was presented as mean ± standard deviation (SD). Two-sample comparisons of means were carried out using the Student's *t*-test. Group means testing was performed using analysis of variance (ANOVA) with Tukey's method for multiple comparisons. Statistical significance was ascertained when p value was less than 0.05.

3. Results and discussion

3.1. Characterization of ZnO nanoparticles

In this study, we evaluated the genotoxic influence of ZnO nanoparticles in relation to the tumor suppressor, p53. Particles were mostly spherical from TEM images (Fig. 1A). These nanoparticles were characterized for their size, shape and surface charges (Fig. 1B). The mean diameter of ZnO nanoparticles was 22.5 ± 4.9 nm, obtained from measurements of 50 nanoparticles using an imaging software (ImageJ). The mean hydrodynamic size of ZnO aggregates in Milli-Q water was found to be about 7.4 times larger than that in complete cell culture medium (DMEM supplemented with 10% FBS, 1% L-glutamine and 1% Antibiotics/Antimycotics) (Fig. 1B). Similar drop in the hydrodynamic size of ZnO nanoparticles in complete medium was reported by Xia et al. [16], suggesting that salts and proteins could help in nanoparticle dispersion in an aqueous environment. The pristine ZnO nanoparticles registered zeta potentials of +14.4 mV. Nanoparticles of differing physicochemical properties such as size, shape and surface charge can exert different cytotoxic effects on cells [2]. From our earlier published work, 13.9% of BEAS-2B cells were found to have internalized the same spherical ZnO nanoparticles used here, introduced at 15 μg/ml, after 4 h incubation [33]. This suggests that these ZnO nanoparticles were able to engage in bioactive interactions with cells and in so doing, could exert both cytotoxic and genotoxic effects.

3.2. Cytotoxicity and genotoxicity of ZnO nanoparticles in RAW264.7 and BEAS-2B

ZnO nanoparticles are being used in a broad range of applications including sunscreens, biosensors, food additives, pigments, rubber additives, and electronic materials [34]. Such extensive use of ZnO nanoparticles does raise safety concerns in the light of growing evidences of their cytotoxic effects [14–17]. This is especially so when our understanding of the biological effects of these ZnO nanoparticles cannot keep up with our ability to manufacture more sophisticated designs in increasing quantities. Here, we show that exposure to increasing concentrations of ZnO nanoparticles decreased the metabolic activity of a mouse macrophage cell line, RAW264.7 (Fig. 2A) in a dose dependent manner after just 24 h of exposure. This is suggestive of a strong cytotoxic effect of ZnO nanoparticles. This trend also held true for ZnO nanoparticles in BEAS-2B, a human bronchial epithelial cell line (Fig. 2B). Estimated LC_{50} concentration of ZnO nanoparticles was about 12.5 μg/ml and 15 μg/ml for RAW264.7 and BEAS-2B, respectively. This significant level of cytotoxicity was in agreement with others who have shown ZnO nanoparticles to be more toxic than other metal oxide based

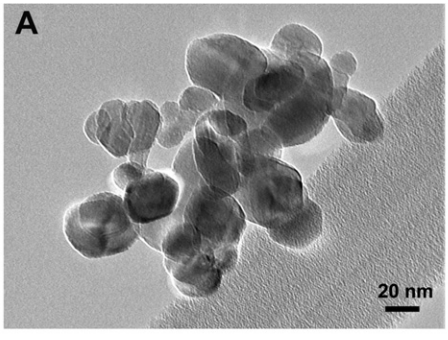

B Physical characterization of ZnO nanoparticles

Sample	Particle size [nm]	Hydrodynamic size [nm]/PDI		Zeta Potential [mV](DI water)
		DI water	DMEM/10% FBS	
ZnO	22.5 ± 4.9	456.5/0.442	61.7/0.14	14.4 ± 1.0

Fig. 1. Physical characterization of nanoparticles. A) TEM micrograph of commercial ZnO nanoparticles. Scale bar: 20 nm. B) Size and surface charge characterization of ZnO nanoparticles in DI water and DMEM containing 10% fetal bovine serum (FBS).

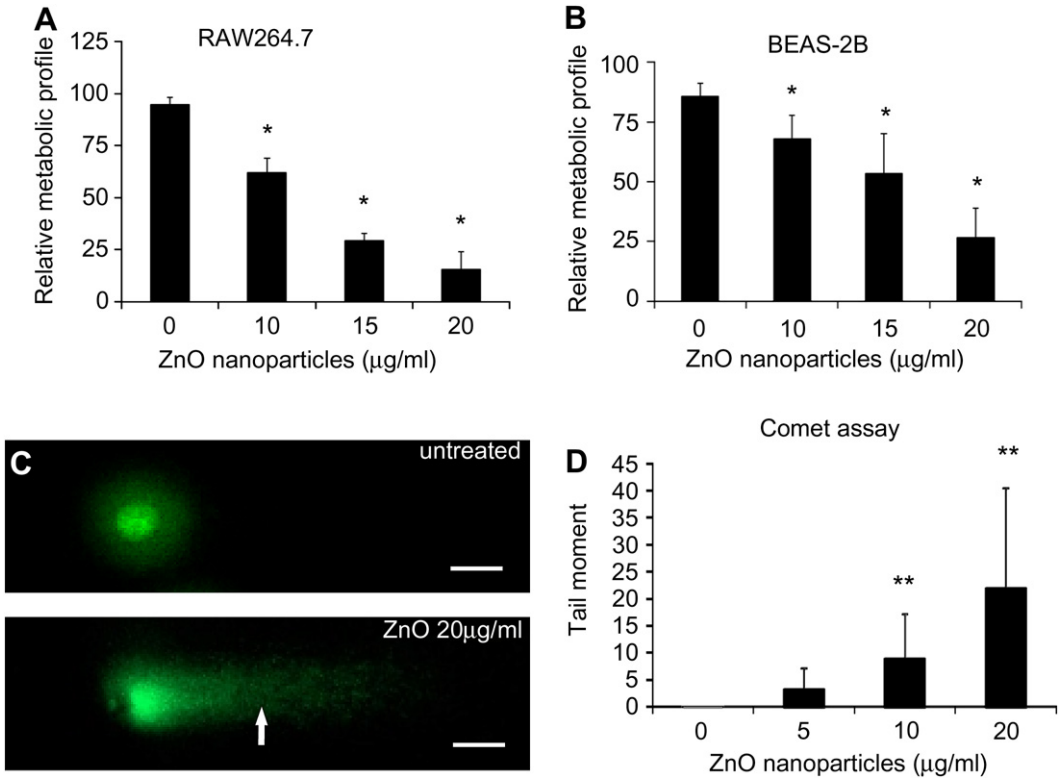

Fig. 2. Cytotoxic and genotoxic effects of ZnO nanoparticles. WST-8 assay performed on A) RAW264.7 and B) BEAS-2B cells showed cytotoxic effects of ZnO nanoparticles in a dose dependent manner after 24 h exposure. Data represent mean ± SD ($n = 3$). *$p < 0.05$ compared to untreated controls. C) DNA damage in BEAS-2B cells was observed using the comet assay. Fluorescent images of encapsulated DNA showed absence of DNA migration in BEAS-2B cultured without nanoparticles (*top panel*) while cells cultured with 20 μg/ml ZnO nanoparticles for 4 h showed clear migrating DNA tails (*bottom panel, arrowhead*). Scale bars: 30 μm. D) Plot of tail moments indicated that there was increasing DNA damage in BEAS-2B cells with increasing ZnO nanoparticle concentration. Data represent mean ± SD ($n = 50$) **$p < 0.01$ compared to untreated control (ANOVA and Tukey's test).

nanoparticles [35]. However, there is another more "sinister" outcome to cytotoxicity of nanoparticles in that DNA damage induced cytotoxicity may also occur due to extended exposure to nanoparticles. Focus was therefore placed on ZnO nanoparticles induced genotoxicity because that poses a more dangerous long term effect of passing mutations to progeny cells that may develop into cancer. Indeed, with the comet assay, ZnO nanoparticles were found to induce an increase in DNA breaks in BEAS-2B cells, in a dose dependent manner (Fig. 2C and D). DNA migration in samples treated with ZnO nanoparticles (10 and 20 μg/ml) was significantly higher than untreated controls ($p < 0.01$, ANOVA and Tukey's test).

3.3. p53 dependent toxicity effects of ZnO nanoparticles

In order to study the role of p53, we compared the effects of ZnO nanoparticle induced DNA damage in wild type and p53 knocked down BJ cells. As expected, we observed a decrease in cell metabolic activity with increasing concentrations of ZnO nanoparticles after 24 h exposure, in both BJ cells (Fig. 3A), especially at high concentrations beyond 15 μg/ml, compared to the control group without any ZnO nanoparticle treatment. This was especially pronounced in WT p53 compared to shp53 BJ cells, presumably a result of p53 induced response to DNA damage caused by ZnO nanoparticles. This showed that the BJ cell lines were sensitive to the cytotoxic effects of ZnO nanoparticle. Metabolic assays by themselves are not directly correlated with cell numbers since the same number of cells of the same cell type may have very different metabolic activities in different environments [36]. To ascertain a firmer idea of cell numbers, we performed DNA quantification (PicoGreen® assay) and observed that there was also a similar trend of decreasing cell numbers with increasing ZnO nanoparticle concentration (Fig. 3B), after 24 h exposure. At 20 and 25 μg/ml ZnO nanoparticle concentrations, there was a significant plunge in total DNA content in the cultures compared to that of lower ZnO nanoparticle concentrations. This drop in cell numbers, especially in WT p53 BJ cells was likely due to DNA damage induced apoptosis, initiated through an intact p53 pathway. Phase contrast images at 20 μg/ml of ZnO nanoparticles reflected the decrease in cell numbers (Fig. 3C) compared to confluent cultures of non-treated controls.

3.4. Role of p53 in ZnO nanoparticles induced toxicity

We next explored the molecular downstream effects of ZnO nanoparticles on p53 signaling pathways in these BJ cells. ZnO nanoparticles at a relatively high concentration of 20 μg/ml resulted in robust phospho-p53 and total p53 levels after 7 days of treatment (Fig. 4A). This was also accompanied by almost negligible levels of phospho-Rb expression at the two serine positions (807 and 811) in samples exposed to 20 μg/ml ZnO nanoparticles (Fig. 4A), suggesting that there was very low cell cycle progression compared to the control. ZnO nanoparticles might be sufficiently genotoxic to stimulate the DNA damage machinery and it might have caused DNA lesions because p53 was upregulated and phosphorylated with a concomitant decrease in cell cycle progression at day 7. The fact that there was a drastic decrease in cell numbers beyond 15 μg/ml ZnO nanoparticle (Fig. 3B) suggests that at lower concentrations, BJ cells were able to accommodate and repair any low abundance DNA damage caused by ZnO nanoparticles. However, this repaired state was quickly overwhelmed at higher ZnO nanoparticle concentrations, resulting in the transition to a pro-apoptosis state.

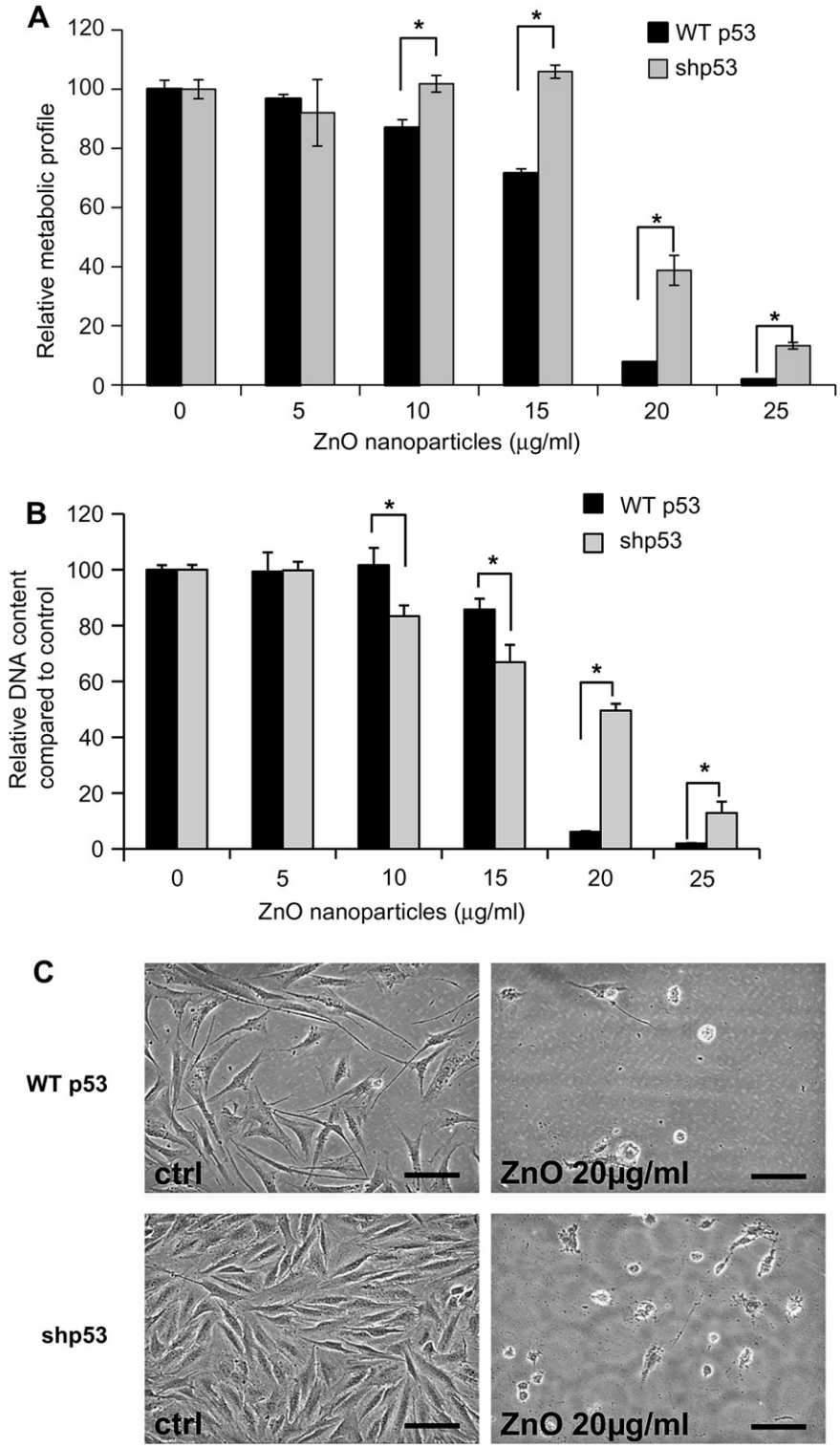

Fig. 3. Differential cytotoxicity of ZnO nanoparticles in BJ cells after 24 h exposure. A) WST-8 assay performed on BJ cells with wild type p53 (WT p53) and knocked down p53 (shp53) and normalized to total DNA amounts. Results showed dose dependent cytotoxic effects of ZnO nanoparticles. In particular, viability of BJ cells in the presence of ZnO nanoparticles dropped drastically at concentrations above 15 μg/ml, which was more significant in WT p53 compared with shp53. Data represent mean ± SD ($n = 3$). *$p < 0.05$. B) PicoGreen® DNA quantification data after 24 h exposure to ZnO nanoparticles reflected increased resistance to DNA damage responses in cells with knocked down p53 levels. Data represent mean ± SD ($n = 3$). *$p < 0.05$. C) Light microscopy images confirmed the trend in cell proliferation shown by DNA quantification, after 24 h exposure to ZnO nanoparticles. Cells were either spindle shaped or had multiple process extensions. In the presence of ZnO nanoparticles, a proportion of cells appeared rounded due to poor viability. Scale bar: 50 μm.

Thereafter we asked whether ZnO nanoparticles induced DNA damage response requires an intact p53 signaling pathway. To answer that, we treated BJ shp53 cells, a p53 knockdown variant of the same parental BJ cell line with ZnO nanoparticles in an increasing dosage. As expected, p53 was not upregulated, proving sufficient knockdown of p53 in that shp53 variant cell line. Interestingly, we saw an upregulation of phosphorylated Rb at serines 807 and 811, at 20 μg/ml ZnO nanoparticle concentration (Fig. 4A),

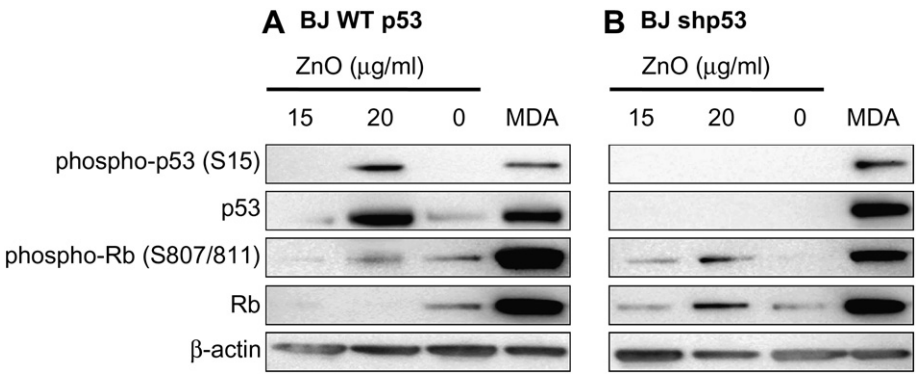

Fig. 4. ZnO nanoparticles elicited a strong p53 dependent DNA damage response. At Day 7 of ZnO nanoparticles exposure at 20 μg/ml, high expression levels of phospho- and total p53 protein was induced in A) BJ cells with wild type p53 (WT p53). As expected, B) BJ cells with knocked down p53 (shp53) did not express any detectable p53 protein. Phospho-Rb was not significantly upregulated in WT p53 group. However, in the shp53 group, there was increased phosphorylation of Rb that might overcome the DNA damage response. MDA-MB-231 (MDA) protein lysate was used as positive controls for immunoblot probing.

which indicated increased cell cycle progression propensity. DNA quantification data showed a more modest decrease in BJ shp53 cell numbers compared to the WT p53 parental line beyond 15 μg/ml of ZnO nanoparticles (Fig. 3B), which could be due to less apoptosis in the situation where p53 levels were drastically reduced. This trend holds true for both higher concentrations of 20 μg/ml and 25 μg/ml ZnO nanoparticles treated BJ shp53 cell line (Fig. 3B) and was also qualitatively observed in the phase contrast light microscopy images of both cell types treated with or without ZnO nanoparticles (Fig. 3C). It was also observed that at the higher concentrations of 10–25 μg/ml ZnO nanoparticles, shp53 showed higher viability than their WT p53 counterpart (Fig. 3A). These data therefore consistently suggest that the degree of DNA damage response towards ZnO nanoparticles depends significantly on an intact p53 pathway.

One of the main modes of how ZnO nanoparticles inflict cellular DNA damage could be through the increased levels of reactive oxygen species (ROS) [16,37] through acidic dissolution of ZnO nanoparticles, possibly in an intra-endosomal reaction. This increased Zn^{2+} ions within the cytoplasmic space trigger ROS generation [16,37]. Interestingly, the molecular mechanism of how Zn^{2+} triggers ROS generation remains unsolved. Nonetheless, restricting Zn^{2+} formation by doping with iron decreases the toxicity of ZnO nanoparticles in a cellular model as well as in mouse, rat and zebrafish *in vivo* models [38]. Taken together, it is suggestive that dissolution of ZnO nanoparticles into ions is an important step in exerting its toxicity effects [39,40]. Whether ROS is the definitive causative perpetrator of DNA damage or some other currently unknown and potentially more sinister and stealthy DNA damage agent remains to be further studied. Whichever the case may be, DNA damage pathways still converge to p53 as the main driver for DNA damage responses and that is what ultimately determines cell fate, prompting us to suggest a hypothetical model of ZnO nanoparticles induced cell death (Fig. 5). Nonetheless, it is noteworthy that even with undetectable p53 expression, shp53 BJ cells, when subjected to the higher concentrations of ZnO

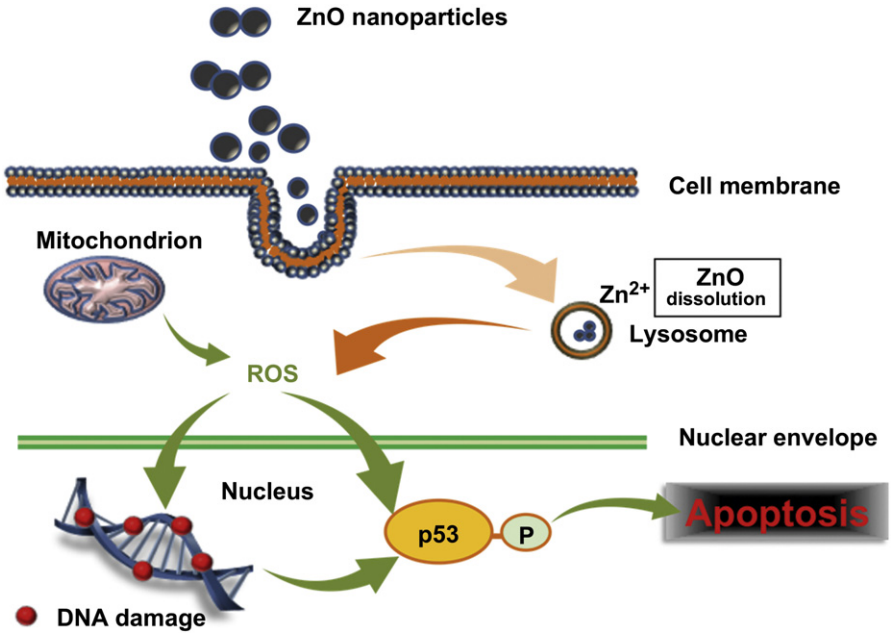

Fig. 5. Proposed cellular response mechanism involving p53 pathway. ZnO nanoparticles underwent extracellular and intracellular dissolution to form Zn^{2+}. Zn^{2+} raises reactive oxygen species (ROS) levels by an unknown mechanism. Increased ROS levels trigger p53 pathway directly or indirectly through DNA damage and the apoptosis machinery is activated. In the event that p53 or its pathway is non-functional, apoptosis is not triggered. (Drawing credits: Tay CY and Leong DT).

nanoparticles (15 and 20 μg/ml, Fig. 3A and B), still experienced significant cell death. This suggested that there is a non-p53 mediated mechanism of cell death that is linked to ZnO nanoparticles. One possible explanation is that ROS generated due to ZnO nanoparticles treatment [40] not only causes DNA damage but also result in extensive cytotoxic membrane damage through lipid peroxidation and protein denaturation. This further undergirded the importance of evaluating the genotoxic effects of other nanoparticles (metal oxides or others) in light of its impingements on the p53 pathway. Such efforts will grow in importance and relevance in the face of the increasing popularity of using nanoparticles in various commercial applications, perhaps using high throughput systems [41] in order to bridge the gulf between the rate at which nano-products are being produced and our understanding of nanotoxicology. One such example, titanium oxide nanoparticles inducing DNA damage in mice [42], also brings into stark focus their potentially carcinogenic long term impact on human health.

Cancers of the lung, esophageal-gastrointestinal tract and skin are among the most common cancers and p53 non-functional mutations are common in those cancers. It is perhaps intuitive that this is so, given that those organs are our first line of defense against the external environment and therefore bear the brunt of external carcinogenic insults. It is worth noting that the anticipated routes of human exposure to nanoparticles (inhalation, ingestion and cutaneous contact) will directly subject these organs to even more genotoxic pressure should the genotoxic effects of nanoparticles be proven significant. In the case of ZnO nanoparticles, potential risks from skin penetration have been extensively discussed because of its widespread use in sunscreens and skin care products [6,43]. Although most evidence available to date favor the notion that the risks of ZnO nanoparticle penetrating across healthy human skin and causing damage are low [44], it has also been noted that the impact of such penetrations through compromised skin had not been adequately addressed by existing studies [6]. Indeed, Mortensen et al. [45] recently demonstrated that penetration of nanoparticles across human skin can be escalated when skin is damaged by UV. This is especially noteworthy given that human keratinocytes are known to have considerable capacity for phagocytosis [46] and that ZnO nanoparticles have been shown to disturb the cell-cycle of keratinocytes [47]. Uptake of ZnO nanoparticles may also occur via passive diffusion through the cell membrane into the cytoplasm [48], independent of the metabolic state of the cell since active transport is not involved. Considering the abundant inclusion of ZnO nanoparticles in sunscreen, our study shows the importance of p53 functional pathway status in skin cells in determining whether ZnO nanoparticles ultimately protects against or accelerates skin cancer.

4. Conclusion

In summary, we evaluated the cytotoxic influence exerted by ZnO nanoparticles on mammalian cells by looking at cell proliferation and cell metabolic profiles after ZnO nanoparticles exposure. We further investigated the genotoxic influence of these nanoparticles in terms of causing DNA damage. Finally, we studied the role of one of the most important tumor suppressors in human cancers, p53, in ZnO nanoparticle induced DNA damage. Our results demonstrated that ZnO nanoparticles are cytotoxic at 10 μg/ml and beyond. In addition, ZnO nanoparticles are capable of causing double-stranded DNA damage. Most significantly, we showed that the genotoxic influence of ZnO nanoparticles resulted in the activation of p53. Furthermore, when p53 function is lost, DNA damage due to ZnO nanoparticles no longer robustly trigger cell death although some cell death still occurred via another mechanism that is not stimulated by DNA damage. Taken collectively, we showed that ZnO nanoparticles may initiate the carcinogenesis process or at least exacerbate any pre-existing carcinogenic situation by failing to trigger apoptosis. Cells lacking p53 may be resistant to ZnO induced apoptosis and develop into cancer. Our study also demonstrates how the genetic background of cells, beyond the intrinsic properties of the nanoparticles, can determine the cytotoxic and genotoxic outcomes.

Acknowledgments

We thank Dr Mathijs Voorhoeve (Duke-NUS Graduate Medical School) for his kind gift of the shRNA retroviral vectors. We also acknowledge Miss Nurulain Binte Khamis for her technical assistance. This work was supported by grants from National Medical Research Council (NMRC-NIG/1002/2009) and Ministry of Education Academic Research Fund (R-364-000-089-112).

References

[1] Nel A, Xia T, Mädler L, Li N. Toxic potential of materials at the nanolevel. Science 2006;311:622–7.
[2] Singh N, Manshian B, Jenkins GJS, Griffiths SM, Williams PM, Maffeis TGG, et al. NanoGenotoxicology: the DNA damaging potential of engineered nanomaterials. Biomaterials 2009;30(23, 24):3891–914.
[3] Obedorster G, Obedorster E, Oberdorster J. Nanotoxicology: an emerging discipline evolving from studies of ultrafine particles. Environ Health Perspect 2005;113:823–39.
[4] Nanotechnology consumer product inventory. Online. Available from URL: http://www.nanotechproject.org/consumerproducts.
[5] Scientific committee on emerging and newly identified health risks. Online. Available from URL: http://ec.europa.eu/health/scientific_committees/emerging/index_en.htm.
[6] Osmond MJ, McCall MJ. Zinc oxide nanoparticles in modern sunscreens: an analysis of potential exposure and hazard. Nanotoxicology 2010;4:15–41.
[7] Pinnell SR, Fairhurst D, Gillies R, Mitchnick MA, Kollias N. Microfine zinc oxide is a superior sunscreen ingredient to microfine titanium dioxide. Dermatol Surg 2000;26:309–14.
[8] Hanley C, Thurber A, Hanna C, Punnoose A, Zhang J, Wingett DG. The influences of cell type and ZnO nanoparticle size on immune cell cytotoxicity and cytokine induction. Nanoscale Res Lett 2009;4:1409–20.
[9] Zhang HJ, Chen BA, Jiang H, Wang CL, Wang HP, Wang XM. A strategy for ZnO nanorod mediated multi-mode cancer treatment. Biomaterials 2011;32(7):1906–14.
[10] Khan Y, Durrani SK, Mehmood M, Ahmad J, Khan M, Firdous S. Low temperature synthesis of fluorescent ZnO nanoparticles. Appl Surf Sci 2010;257:1756–61.
[11] Liu YL, Ai KL, Yuan QH, Lu LH. Fluorescence-enhanced gadolinium-doped zinc oxide quantum dots for magnetic resonance and fluorescence imaging. Biomaterials 2011;32(4):1185–92.
[12] Zhang P, Liu WG. ZnO QD@PMAA-co-PDMAEMA nonviral vector for plasmid DNA delivery and bioimaging. Biomaterials 2010;31(11):3087–94.
[13] Rasmussen JW, Martinez E, Louka P, Wingett DG. Zinc oxide nanoparticles for selective destruction of tumor cells and potential for drug delivery applications. Expert Opin Drug Deliv 2010;7:1063–77.
[14] Heng BC, Zhao X, Xiong S, Ng KW, Boey FYC, Loo JSC. Cytotoxicity of zinc oxide (ZnO) nanoparticles is influenced by cell density and culture format. Arch Toxicol 2010;85:695–704.
[15] Heng BC, Zhao X, Xiong S, Ng KW, Boey FYC, Loo JSC. Toxicity of zinc oxide (ZnO) nanoparticles on human bronchial epithelial cells (BEAS-2B) is accentuated by oxidative stress. Food Chem Toxicol 2010;48:1762–6.
[16] Xia T, Kovochich M, Liong M, Mädler L, Gilbert B, Shi H, et al. Comparison of the mechanism of toxicity of zinc oxide and cerium oxide nanoparticles based on dissolution and oxidative stress properties. ACS Nano 2008;2:2121–34.
[17] Yuan JH, Chen Y, Zha HX, Song LJ, Li CY, Li JQ, et al. Determination, characterization and cytotoxicity on HELF cells of ZnO nanoparticles. Colloids Surf B Biointerfaces 2010;76:145–50.
[18] Sharma V, Shukla RK, Saxena N, Parmar D, Das M, Dhawan A. DNA damaging potential of zinc oxide nanoparticles in human epidermal cells. Toxicol Lett 2009;185:211–8.
[19] Yin H, Casey PS, McCall MJ, Fenech M. Effects of surface chemistry on cytotoxicity, genotoxicity, and the generation of reactive oxygen species induced by ZnO nanoparticles. Langmuir 2010;26:15399–408.
[20] Ciccia A, Elledge SJ. The DNA damage response: making it safe to play with knives. Mol Cell 2010;40:179–204.
[21] Hoeijmakers JHJ. DNA damage, aging, and cancer. N Engl J Med 2009;361:1475–85.
[22] Hollstein M, Sidransky D, Vogelstein B, Harris CC. p53 mutations in human cancers. Science 1991;253:49–53.

[23] Cho Y, Gorina S, Jeffrey PD, Pavletich NP. Crystal structure of a p53 tumor suppressor-DNA complex: understanding tumorigenic mutations. Science 1994;265:346–55.
[24] Ahamed M, Akhtar MJ, Raja M, Ahmad I, Siddiqui MK, Alsalhi MS, et al. ZnO nanorod-induced apoptosis in human alveolar adenocarcinoma cells via p53, survivin and bax/bcl-2 pathways: role of oxidative stress. Nanomedicine; 2011. doi:10.1016/j.nano.2011.04.011.
[25] Raschke WC, Baird S, Ralph P, Nakoinz I. Functional macrophage cell lines transformed by Abelson leukemia virus. Cell 1978;15:261–7.
[26] Reddel RR, Ke Y, Gerwin BI, McMenamin MG, Lechner JF, Su RT, et al. Transformation of human bronchial epithelial cells by infection with SV40 or adenovirus-12 SV40 hybrid virus, or transfection via strontium phosphate coprecipitation with a plasmid containing SV40 early region genes. Cancer Res 1988;48:1904–9.
[27] Gazdar AF, Butel JS, Carbone M. SV40 and human tumours: myth, association or causality? Nat Rev Cancer 2002;2:957–64.
[28] Drost J, Mantovani F, Tocco F, Elkon R, Comel A, Holstege H, et al. BRD7 is a candidate tumour suppressor gene required for p53 function. Nat Cell Biol 2010;12:380–9.
[29] Kortlever RM, Higgins PJ, Bernards R. Plasminogen activator inhibitor-1 is a critical downstream target of p53 in the induction of replicative senescence. Nat Cell Biol 2006;8:877–84.
[30] Voorhoeve PM, Agami R. The tumor-suppressive functions of the human INK4A locus. Cancer Cell 2003;4:311–9.
[31] Brummelkamp TR, Bernards R, Agami RA. System for stable expression of short interfering RNAs in mammalian cells. Science 2002;296:550–3.
[32] Olive PL, Banath JP. The comet assay: a method to measure DNA damage in individual cells. Nat Protoc 2006;1:23–9.
[33] Heng BC, Zhao XX, Tan EC, Khamis N, Assodani A, Xiong SJ, et al. Evaluation of the cytotoxic and inflammatory potential of differentially-shaped zinc oxide nanoparticles. Arch Toxicol; 2011. doi:10.1007/s00204-011-0722-1.
[34] Brayner R, Dahoumane SA, Yéprémian C, Djediat C, Meyer M, Couté A, et al. ZnO nanoparticles: synthesis, characterization, and ecotoxicological studies. Langmuir 2010;26:6522–8.
[35] Puzyn T, Rasulev B, Gajewicz A, Hu X, Dasari TP, Michalkova A, et al. Using nano-QSAR to predict cytotoxicity of metal oxide nanoparticles. Nat Nanotechnol 2011;6:175–8.
[36] Ng KW, Leong DT, Hutmacher DW. The challenge to measure cell proliferation in two and three dimensions. Tissue Eng 2005;11:182–91.
[37] Muller KH, Kulkarni J, Motskin M, Goode A, Winship P, Skepper JN, et al. pH-dependent toxicity of high aspect ratio ZnO nanowires in macrophages due to intracellular dissolution. ACS Nano 2010;4:6767–79.
[38] Xia T, Zhao Y, Sager T, George S, Pokhrel S, Li N, et al. Decreased dissolution of ZnO by iron doping yields nanoparticles with reduced toxicity in the rodent lung and zebrafish embryos. ACS Nano 2011;5:1223–35.
[39] Wätjen W, Haase H, Biagioli M, Beyersmann D. Induction of apoptosis in mammalian cells by cadmium and zinc. Environ Health Perspect 2002;110-(Suppl):865–7.
[40] George S, Pokhrel S, Xia T, Gilbert B, Ji Z, Schowalter M, et al. Use of a rapid cytotoxicity screening approach to engineer a safer zinc oxide nanoparticle through iron doping. ACS Nano 2010;4:15–29.
[41] Meng H, Xia T, George S, Nel AE. A predictive toxicological paradigm for the safety assessment of nanomaterials. ACS Nano 2009;3:1620–7.
[42] Trouiller B, Reliene R, Westbrook A, Solaimani P, Schiestl RH. Titanium dioxide nanoparticles induce DNA damage and genetic instability in vivo in mice. Cancer Res 2009;69:8784–9.
[43] Borm PJA, Robbins D, Haubold S, Kuhlbusch T, Fissan H, Donaldson K, et al. The potential risks of nanomaterials: a review carried out for ECETOC. Part FIbre Toxicol 2006;3:11.
[44] Nohynek GJ, Dufour EK, Roberts MS. Nanotechnology, cosmetics and the skin: is there a health risk? Skin Pharmacol Physiol 2008;21:136–49.
[45] Mortensen LJ, Oberdörster G, Pentland AP, Delouise LA. in vivo skin penetration of quantum dot nanoparticles in the murine model: the effect of UVR. Nano Lett 2008;8:2779–87.
[46] Korting HC, Zienicke H, Schäfer-Korting M, Braun-Falco O. Liposome encapsulation improves efficacy of betamethasone dipropionate in atopic eczema but not in psoriasis vulgaris. Eur J Clin Pharmacol 1990;39:349–51.
[47] Kocbek P, Teskac K, Kreft ME, Kristl J. Toxicological aspects of long-term treatment of keratinocytes with ZnO and TiO2 nanoparticles. Small 2010;6: 1908–17.
[48] Geiser M, Rothen-Rutishauser B, Kapp N, Schürch S, Kreyling W, Schulz H, et al. Ultrafine particles cross cellular membranes by nonphagocytic mechanisms in lungs and in cultured cells. Environ Health Perspect 2005;113: 1555–60.